Int. J. Solids Structures Vol. 30, No. 22, pp. 3171–3184, 1993
Printed in Great Britain

0020–7683/93 $6.00+ .00
Pergamon Press Ltd

A NEW MODEL OF GENERALIZED PLASTICITY AND ITS NUMERICAL IMPLEMENTATION

J. LUBLINER, R. L. TAYLOR and F. AURICCHIO
Department of Civil Engineering, University of California at Berkeley,
Berkeley, CA 94720, U.S.A.

(*Received* 11 *August* 1992; *in revised form* 25 *March* 1993)

Abstract—A previously proposed simple model of generalized plasticity is modified so that it allows behavior that is asymptotically perfectly plastic or strain-softening. Initially presented in uniaxial form, the model is then generalized to multiaxial stress. Numerical implementation is developed first through direct integration of the rate equations, including special cases in which the solution may be obtained analytically, and then by means of a return-map algorithm, which is particularly well suited to the finite-element method; consistent algorithmic tangent moduli are derived as well. Numerical examples are presented to illustrate the various approaches.

1. INTRODUCTION

Generalized plasticity is a model developed by one of the authors (JL) as, first, the result of an axiomatic approach to inelastic behavior described by internal variables (Lubliner, 1974, 1975, 1980, 1984), and second, as a practical way of describing observed behavior of solids which unload elastically when loaded into the plastic range but in which, upon reloading, renewed plasticity begins before the attainment of the stress where unloading began (see Fig. 1). To this end, some simple models were proposed (Lubliner, 1981, 1989, 1991). In the model discussed in the last-named reference, the relation between the plastic strain ε^p and the stress σ upon initial loading in uniaxial stress is governed by

$$\frac{d\varepsilon^p}{d\sigma} = \frac{1}{H\beta}\langle\sigma - \sigma_Y - H\varepsilon^p\rangle. \tag{1}$$

Here $\langle\cdot\rangle$ is the Macauley bracket, σ_Y is the initial yield stress, and H [denoted α in Lubliner (1991)] and β are two additional positive constants with the dimensions of stress. The resulting stress–strain curve is asymptotic to the line $\sigma = \sigma_Y + \beta + H\varepsilon^p$, so that H is the asymptotic plastic modulus, and β is the displacement in the stress direction between the asymptote and the line $\sigma = \sigma_Y + H\varepsilon^p$ representing the yield surface. The limit $\beta = 0$ represents classical plasticity, that is, the stress remains on the yield surface. However, the limit

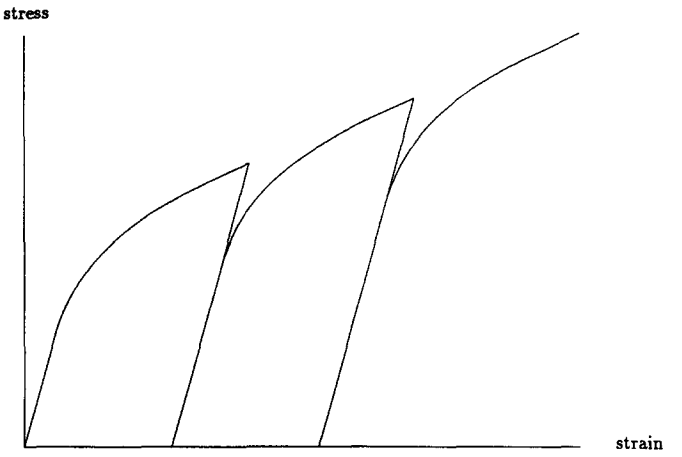

Fig. 1. Stress–strain loading–unloading–reloading diagram motivating general plasticity.

as $H \to 0$ is singular, in that the solution is $\sigma = \sigma_Y$ independent of β; consequently, the model is limited to work-hardening solids. If eqn (1) is modified by replacing H in the denominator on the right-hand side by some other constant, say R, then the limiting curve as $H \to 0$ is the parabola $\sigma = \sigma_Y + \sqrt{2R\beta\varepsilon^p}$. Numerical implementation of the model when H is small (though positive) leads to curves that overshoot the asymptote, confirming the singularity.

It may be noted that the derivation of a stress–strain curve that is asymptotic to a straight line is the goal of the many "two-surface" models that have been presented in the past 15 years or so. The simple generalized plasticity model achieves this without any special assumptions.

In the present paper, a modification of the just-described model, which eliminates the disadvantages of the model described by eqn (1), is presented in Section 2 in both a uniaxial and a multiaxial formulation. In Section 3 certain simple problems are solved by direct integration of the rate equation, which in some cases results in a closed-form solution that can be used to test other solution methods. Section 4 shows how the return-mapping algorithm can be used to solve problems governed by the proposed model in a finite-element setting.

2. NEW MODEL

2.1. *Uniaxial formulation*

The disadvantages presented by eqn (1) can be eliminated by postulating the following equation in its place:

$$\frac{d\varepsilon^p}{d\sigma} = \frac{\langle \sigma - \sigma_Y - H\varepsilon^p \rangle}{H\beta + R[\beta - (\sigma - \sigma_Y - H\varepsilon^p)]}, \tag{2}$$

where H and β have the same meaning as before, and R is a positive constant with the dimensions of stress. Upon defining $u = (\sigma - \sigma_Y - H\varepsilon^p)/\beta$, eqn (2) can be solved explicitly for σ and ε^p in terms of u, and if $h \overset{\text{def}}{=} H/R$ then the resulting initial loading curve is given parametrically by

$$\begin{aligned} \frac{R\varepsilon^p}{\beta} &= \frac{1}{1+h}\left(\ln\frac{1}{1-u} - u\right), \\ \frac{\sigma - \sigma_Y}{\beta} &= \frac{1}{1+h}\left(h\ln\frac{1}{1-u} + u\right), \end{aligned} \tag{3}$$

for $0 \leqslant u < 1$, provided $h > -1$. The fact that H can be negative means that the model can describe even stress–strain curves whose asymptotes represent softening; see, for example, Fig. 2, showing dimensionless loading–unloading–reloading diagrams (for $H = -0.1E$, $E = R$, and $\sigma_Y = \beta$).

As in the preceding model, the plastic modulus H can be decomposed into a kinematic part H' and an isotropic part H'', with $H = H' + H''$, and a yield function f defined by

$$f = |\sigma - H'\varepsilon^p| - \sigma_Y - H''\kappa, \tag{4}$$

where κ is the isotropic hardening variable defined by $d\kappa = |d\varepsilon^p|$. Note that unlike eqn (8) of Lubliner (1991), the yield function defined by eqn (4) is not dimensionless but has dimensions of stress. For arbitrary loadings, then, eqn (1) may be replaced by

$$\dot{\varepsilon}^p = \phi \operatorname{sgn}(\sigma - H'\varepsilon^p)\langle \operatorname{sgn}(\sigma - H'\varepsilon^p)\dot{\sigma} \rangle, \tag{5}$$

where

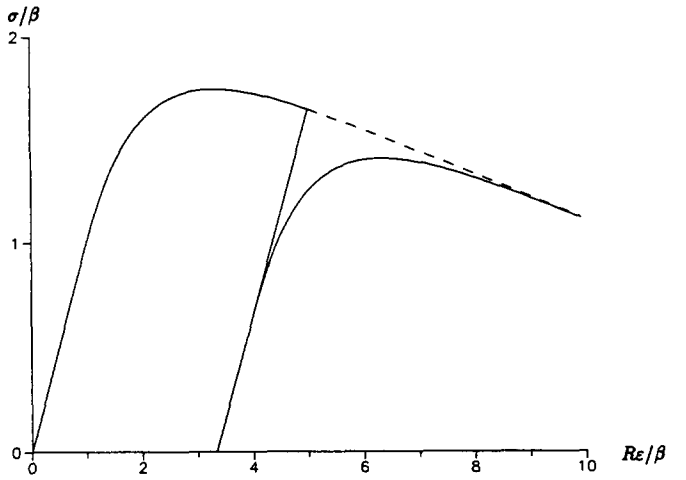

Fig. 2. Loading–unloading–reloading diagram for a softening material ($H = -0.1E$).

$$\phi = \frac{\langle f \rangle}{H\beta + R(\beta - f)}, \tag{6}$$

replacing eqn (4) of Lubliner (1991).

2.2. *Generalization to multiaxial stress*

The generalization of the yield function f to multiaxial stress states is

$$f = \tilde{\sigma} - \sigma_Y - H''\kappa, \tag{7}$$

where κ and $\tilde{\sigma}$ are defined by

$$\dot{\kappa} = |\dot{\boldsymbol{\varepsilon}}^p|, \quad \tilde{\sigma} = |\boldsymbol{\sigma} - \tfrac{2}{3}H'\boldsymbol{\varepsilon}^p|',$$

with the definitions of the norm $|\cdot|$ in strain-rate space and of the seminorm $|\cdot|'$ in stress space depending on the yield criterion selected. The corresponding generalization of eqn (5), with an associated flow rule assumed, is

$$\dot{\boldsymbol{\varepsilon}}^p = \phi \boldsymbol{v} \langle \boldsymbol{v} : \dot{\boldsymbol{\sigma}} \rangle, \tag{8}$$

where ϕ is defined by eqn (6) and

$$\boldsymbol{v} = \frac{\partial f / \partial \boldsymbol{\sigma}}{|\partial f / \partial \boldsymbol{\sigma}|}.$$

For the von Mises and Tresca yield criteria, $|\cdot|$ and $|\cdot|'$ are defined as follows:

$$|\dot{\boldsymbol{\varepsilon}}^p| = \sqrt{\tfrac{2}{3}\dot{\varepsilon}^p_{ij}\dot{\varepsilon}^p_{ij}}, \qquad |\tilde{\boldsymbol{\sigma}}|' = \sqrt{\tfrac{3}{2}\tilde{s}_{ij}\tilde{s}_{ij}}, \qquad \text{von Mises},$$

$$|\dot{\boldsymbol{\varepsilon}}^p| = \tfrac{1}{2}(|\dot{\varepsilon}^p_1| + |\dot{\varepsilon}^p_2| + |\dot{\varepsilon}^p_3|), \quad |\tilde{\boldsymbol{\sigma}}|' = \tfrac{1}{2}(|\tilde{\sigma}_1 - \tilde{\sigma}_2| + |\tilde{\sigma}_2 - \tilde{\sigma}_3| + |\tilde{\sigma}_1 - \tilde{\sigma}_3|), \quad \text{Tresca},$$

where $\tilde{\mathbf{s}}$ is the deviator of $\tilde{\boldsymbol{\sigma}} \overset{\text{def}}{=} \boldsymbol{\sigma} - \frac{2}{3}H'\boldsymbol{\varepsilon}^p$, and where the subscripts in the Tresca case refer to principal-axis components. Consequently, for the von Mises case $\boldsymbol{v}$ is given by

$$\boldsymbol{v} = \frac{3}{2\tilde{\sigma}}\tilde{\mathbf{s}}, \tag{9}$$

while in the Tresca case

$$v_1 = \tfrac{1}{2}[\operatorname{sgn}(\tilde{\sigma}_1 - \tilde{\sigma}_2) + \operatorname{sgn}(\tilde{\sigma}_1 - \tilde{\sigma}_2)],$$
$$v_2 = \tfrac{1}{2}[\operatorname{sgn}(\tilde{\sigma}_2 - \tilde{\sigma}_3) + \operatorname{sgn}(\tilde{\sigma}_2 - \tilde{\sigma}_1)],$$
$$v_3 = \tfrac{1}{2}[\operatorname{sgn}(\tilde{\sigma}_3 - \tilde{\sigma}_1) + \operatorname{sgn}(\tilde{\sigma}_3 - \tilde{\sigma}_2)].$$

It can be shown that the parametric representation of the σ–ε^p relation given by eqns (3) for initial uniaxial loading can be generalized to a relation between $\tilde{\sigma}$ and κ under arbitrary loading. The discussion will be limited to the von Mises criterion. It follows from eqn (8) and the preceding definitions that

$$\dot{\kappa} = \phi\langle \boldsymbol{v} : \dot{\boldsymbol{\sigma}} \rangle. \tag{10}$$

Since $\boldsymbol{v}$ is purely deviatoric, it follows that $\boldsymbol{v} : \dot{\boldsymbol{\sigma}} = \boldsymbol{v} : \dot{\mathbf{s}}$, and hence, from the definition of $\tilde{\mathbf{s}}$,

$$\dot{\kappa} = \phi\langle \boldsymbol{v} : (\dot{\tilde{\mathbf{s}}} + \tfrac{2}{3}H'\dot{\boldsymbol{\varepsilon}}^p) \rangle.$$

But

$$\boldsymbol{v} : \dot{\tilde{\mathbf{s}}} = \dot{\tilde{\sigma}}, \quad \tfrac{2}{3}\boldsymbol{v} : \dot{\boldsymbol{\varepsilon}}^p = \dot{\kappa}.$$

Therefore

$$\dot{\kappa} = \phi\langle \dot{\tilde{\sigma}} + H'\dot{\kappa} \rangle,$$

so that

$$\dot{\kappa} = \frac{\phi}{1 - H'\phi}\langle \dot{\tilde{\sigma}} \rangle. \tag{11}$$

Introducing, as before, $u = f/\beta$, with f given by (7), and noting that $\dot{\tilde{\sigma}} = \beta\dot{u} + H''\dot{\kappa}$, one is led finally to

$$\dot{\kappa} = \frac{b}{1+h}\frac{\langle u \rangle}{1-u}\langle \dot{u} \rangle, \tag{12}$$

where $b = \beta/R$. In problems in which $\dot{u} \geqslant 0$, this equation may be integrated to give

$$\kappa = \frac{b}{1+h}\left(\ln\frac{1}{1-u} - u\right), \quad u \geqslant 0, \tag{13}$$

and correspondingly,

$$\tilde{\sigma} = \sigma_Y + \frac{\beta}{1+h}\left[h'' \ln\frac{1}{1-u} + (1+h')u\right], \tag{14}$$

where $h' = H'/R$, $h'' = H''/R$.

3. DIRECT INTEGRATION OF THE RATE EQUATIONS

3.1. *Special case: purely isotropic hardening under stress control*

The integration of the rate equations becomes especially simple in the case of purely isotropic hardening ($H' = 0$, $H'' = H$) under stress control. In this case $\tilde{\boldsymbol{\sigma}} = \boldsymbol{\sigma}$, so that

$|\boldsymbol{\sigma}|' = \tilde{\sigma}$, which is determined by u. Thus if an increment du is given, $d\kappa$ and $d\tilde{\sigma}$ are determined, and if the direction of the stress increment $d\boldsymbol{\sigma}$ is given by $\boldsymbol{\omega}$, that is, $d\boldsymbol{\sigma} = \boldsymbol{\omega}\, d\tilde{\sigma}$, where $\tilde{\sigma}$ is defined by

$$d\tilde{\sigma} = |d\boldsymbol{\sigma}|',$$

then

$$\tfrac{2}{3}\tilde{\sigma}\, d\tilde{\sigma} = \mathbf{s} : d\mathbf{s} = \mathbf{s} : d\boldsymbol{\sigma} = \mathbf{s} : \boldsymbol{\omega}\, d\tilde{\sigma},$$

so that

$$d\boldsymbol{\sigma} = \frac{2}{3}\boldsymbol{\omega}\frac{\tilde{\sigma}\, d\tilde{\sigma}}{\mathbf{s} : \boldsymbol{\omega}}, \tag{15}$$

(provided $\mathbf{s} : \boldsymbol{\omega} \neq 0$; the case $\mathbf{s} : \boldsymbol{\omega} = 0$ means that instantaneously $d\tilde{\sigma} = 0$), while the plastic strain increment is

$$d\boldsymbol{\varepsilon}^{\mathrm{p}} = \frac{3\mathbf{s}}{2\tilde{\sigma}} d\kappa,$$

so that the total strain-deviator increment is given by

$$d\mathbf{e} = \frac{1}{2G} d\mathbf{s} + \frac{3\mathbf{s}}{2\tilde{\sigma}} d\kappa,$$

and the determination of the strain is reduced to integration.

As an example, we consider the problem of a thin-walled circular tube that is first loaded by an axial force and then by a gradually increasing torque, while the axial force remains constant. With no internal or external pressure, the state of stress may be assumed to consist of an axial normal stress σ and a shear stress τ, and the only strain components that need to be considered are the axial normal strain ε and the shear strain γ. For the case of pure torsion, with $\sigma = 0$, the solution may be obtained from the uniaxial case described by eqns (3) by substituting $\gamma^{\mathrm{p}}/\sqrt{3}$ for ε^{p} and $\sqrt{3}\tau$ for σ. With σ different from zero, the plastic strain increments are given by

$$d\varepsilon^{\mathrm{p}} = \frac{\sigma}{\tilde{\sigma}} d\kappa,$$

$$d\gamma^{\mathrm{p}} = \frac{3\tau}{\tilde{\sigma}} d\kappa, \tag{16}$$

and $d\kappa$ may be obtained from eqn (13) as

$$d\kappa = \frac{b}{1+h}\frac{u}{1-u} du.$$

Moreover, $\tilde{\sigma} = \sqrt{\sigma^2 + 3\tau^2}$ is given as a function of u (for $u \geqslant 0$) by the right-hand side of eqn (14) with $h'' = h$ and $h' = 0$, that is

$$\tilde{\sigma} = \sigma_{\mathrm{Y}} + \frac{\beta}{1+h}\left(h \ln \frac{1}{1-u} + u\right),$$

and $\tau = \sqrt{(\tilde{\sigma}^2 - \sigma^2)/3}$. Since σ is constant, the right-hand sides of eqns (16) may be expressed as functions of u times du and integrated accordingly. For $\sigma \leqslant \sigma_{\mathrm{Y}}$, the initial value of u is zero; for $\sigma > \sigma_{\mathrm{Y}}$ it is given implicitly by eqn $(3)_2$. The integration is simplified if the integration variable is changed from u to $v = \ln [1/(1-u)]$. Some results, obtained by means

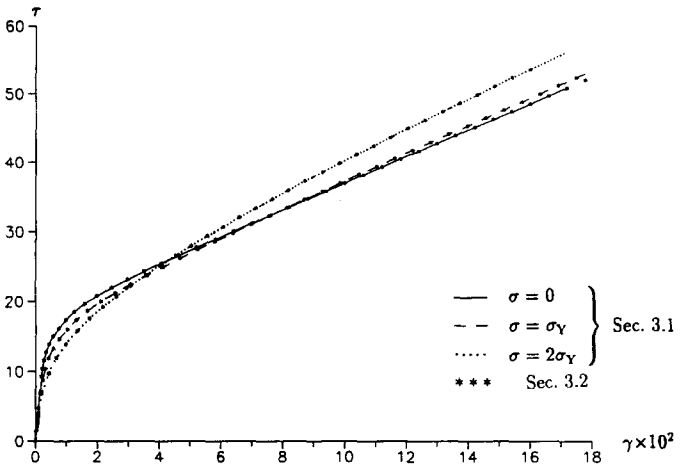

Fig. 3. Torsion of a thin-walled tube under constant axial force, purely isotropic hardening.

of the trapezoidal rule with $\Delta v = 0.001$, are shown in Fig. 3 as plots of τ against γ (where $\gamma = \gamma^{\mathrm{p}} + \tau/G$) for $\sigma = 0$ (solid line), $\sigma = \sigma_{\mathrm{Y}}$ (dashed line) and $\sigma = 2\sigma_{\mathrm{Y}}$ (dotted line); the values of the material parameters (in arbitrary stress units) are $G = 5000$, $H = 600$, $R = 2000$, $\beta = 16$ and $\sigma_{\mathrm{Y}} = 16$.

3.2. *The general case: comparison with previous solution*

In the presence of kinematic hardening, or under strain control (or mixed control), the right-hand side of the equation for $\mathrm{d}\varepsilon^{\mathrm{p}}$ contains ε^{p}, so that the problem is one of solving a set of possibly coupled nonlinear differential equations. The preceding special case, for which an explicit solution is available, may be used to test solution methods.

Provided $\tilde{\sigma}$ is no less than σ_{Y} and is not decreasing, eqn (11) may be written in the form

$$\frac{\mathrm{d}\kappa}{\mathrm{d}\tilde{\sigma}} = \Phi(\tilde{\sigma}, \kappa), \tag{17}$$

where Φ is defined by eqn (11) and is given explicitly, as a result of eqns (6) and (7), by

$$\Phi = \frac{\langle \tilde{\sigma} - \sigma_{\mathrm{Y}} - H''\kappa \rangle}{H''\beta + (R + H')(\beta - \tilde{\sigma} + \sigma_{\mathrm{Y}} + H''\kappa)}. \tag{18}$$

With $\tilde{\sigma}$ as the independent variable, the differential equations may be solved by the generalized Euler method, namely,

$$\kappa_{i+1} - \kappa_i = (1-\alpha)\Phi(\tilde{\sigma}_i, \kappa_i) + \alpha\Phi(\tilde{\sigma}_{i+1}, \kappa_{i+1}),$$

where $\alpha = 0$, $\frac{1}{2}$ and 1 correspond respectively to the classical (forward or explicit) Euler method, the trapezoid method and the backward Euler method [see, e.g., Dahlquist and Björck (1974)]. For $\alpha > 0$, the equation may be solved for κ_{i+1} if the second term on the right-hand side is approximated by

$$\Phi(\tilde{\sigma}_{i+1}, \kappa_{i+1}) = \Phi(\tilde{\sigma}_{i+1}, \kappa_i) + \Phi_\kappa(\tilde{\sigma}_{i+1}, \kappa_i)(\kappa_{i+1} - \kappa_i),$$

where $\Phi_\kappa = \partial\Phi/\partial\kappa$. When $H'' = H$, $\tilde{\sigma} = \sqrt{3}\tau$ and $\kappa = \gamma^{\mathrm{p}}/\sqrt{3}$, the problem corresponds to that of simple shear, as in the previously treated pure torsion of a thin-walled tube, and may be compared with the previous solution.

The problem of torsion under a constant axial force requires the additional relations (16), but they present no difficulty, since eqn (17) may first be solved independently. Computation with increments in $\tilde{\sigma}$ of 0.1 yields results that are virtually independent of α—that is, the use of implicit methods presents no discernible improvement over the forward Euler method. The results are shown as asterisks in Fig. 3; as can be seen, they are virtually indistinguishable from those obtained by numerical integration.

3.3. *Combined hardening under stress control*

If $H' \neq 0$, then $\tilde{\sigma}$ is no longer determined by the stress alone and becomes a dependent variable, along with κ and ε^p. Under stress control, $\bar{\sigma}$ can be used as the control variable, and the relations between the increments in the dependent variables and those in $\bar{\sigma}$ are given by the coupled differential equations consisting, first, of

$$\frac{d\tilde{\sigma}}{d\bar{\sigma}} = \frac{3\langle(\mathbf{s}-\frac{2}{3}H'\boldsymbol{\varepsilon}^p):\boldsymbol{\omega}\rangle}{2(1+H'\Phi)\tilde{\sigma}} \stackrel{\text{def}}{=} \Psi(\mathbf{s}, \bar{\sigma}, \boldsymbol{\varepsilon}^p, \kappa), \tag{19}$$

where $\boldsymbol{\omega}$ denotes, as before, the direction of $d\boldsymbol{\sigma}$ and is assumed known. Combining eqns (17) and (19) yields, next,

$$\frac{d\kappa}{d\bar{\sigma}} = \Phi\Psi \stackrel{\text{def}}{=} \Theta(\mathbf{s}, \tilde{\sigma}, \kappa, \boldsymbol{\varepsilon}^p), \tag{20}$$

and the flow rule gives, finally,

$$\frac{d\boldsymbol{\varepsilon}^p}{d\bar{\sigma}} = \frac{3\Phi\Psi}{2\tilde{\sigma}}(\mathbf{s}-\tfrac{2}{3}H'\boldsymbol{\varepsilon}^p) \stackrel{\text{def}}{=} \boldsymbol{\Omega}(\mathbf{s}, \tilde{\sigma}, \kappa, \boldsymbol{\varepsilon}^p). \tag{21}$$

Equations (19)–(21) constitute a coupled set of nonlinear ordinary differential equations for the unknown variables $\tilde{\sigma}$, κ, $\boldsymbol{\varepsilon}^p$, with $\bar{\sigma}$ as the control variable.

In the example of the thin-walled tube twisted under a constant axial force, the problem may be formulated in terms of the unknown variables $\tilde{\sigma}$, κ and γ^p, with τ as the control variable (note that if $d\sigma = 0$ then $d\bar{\sigma} = \sqrt{3}\,d\tau$, but it is more convenient to work directly with τ). With the definitions

$$\mu \stackrel{\text{def}}{=} \frac{1}{1+H'\Phi} = \frac{H''\beta+(R+H')(\beta-\tilde{\sigma}+\sigma_Y+H''\kappa)}{H\beta+R(\beta-\tilde{\sigma}+\sigma_Y+H''\kappa)}$$

and

$$\tilde{\tau} \stackrel{\text{def}}{=} \tau - \tfrac{1}{3}H'\gamma^p,$$

the equations are

$$\begin{aligned}
\frac{d\tilde{\sigma}}{d\tau} &= \frac{3\tilde{\tau}\mu}{\tilde{\sigma}} \stackrel{\text{def}}{=} \psi(\tau, \tilde{\sigma}, \kappa, \gamma^p),\\
\frac{d\kappa}{d\tau} &= \psi(\tau, \tilde{\sigma}, \kappa, \gamma^p)\Phi(\tilde{\sigma}, \kappa) \stackrel{\text{def}}{=} \theta(\tau, \tilde{\sigma}, \kappa, \gamma^p),\\
\frac{d\gamma^p}{d\tau} &= \frac{3\tilde{\tau}}{\tilde{\sigma}}\theta(\tau, \tilde{\sigma}, \kappa, \gamma^p) \stackrel{\text{def}}{=} \chi(\tau, \tilde{\sigma}, \kappa, \gamma^p).
\end{aligned} \tag{22}$$

It is clear that the equations are coupled. However, while $\boldsymbol{\varepsilon}^p$ is contained in $\tilde{\sigma}$, it does not appear explicitly in eqns (22). In fact, at each step of the solution, $\boldsymbol{\varepsilon}^p$ may be calculated by means of the relation

$$\sigma = \sqrt{(\sigma - H'\varepsilon^p)^2 + 3(\tau - \tfrac{1}{3}H'\gamma^p)^2},$$

that is,

$$\varepsilon^p = \frac{1}{H'}[\sigma - \sqrt{\tilde{\sigma}^2 - 3(\tau - \tfrac{1}{3}H'\gamma^p)^2}].$$

The numerical solutions of eqns (22) by any implicit method require the evaluation of the partial derivatives of ψ, θ and χ with respect to $\tilde{\sigma}$, κ and γ^p. These may be defined as follows:

$$\begin{bmatrix} \frac{\partial\psi}{\partial\tilde{\sigma}} & \frac{\partial\psi}{\partial\kappa} & \frac{\partial\psi}{\partial\gamma^p} \\ \frac{\partial\theta}{\partial\tilde{\sigma}} & \frac{\partial\theta}{\partial\kappa} & \frac{\partial\theta}{\partial\gamma^p} \\ \frac{\partial\chi}{\partial\tilde{\sigma}} & \frac{\partial\chi}{\partial\kappa} & \frac{\partial\chi}{\partial\gamma^p} \end{bmatrix} = - \begin{bmatrix} \left(\frac{1}{\tilde{\sigma}} + H'\mu\Phi_{\tilde{\sigma}}\right)\psi & H'\mu\Phi_\kappa\psi & \frac{H'\mu}{\tilde{\sigma}} \\ \left(\frac{\Phi}{\tilde{\sigma}} - \mu\Phi_{\tilde{\sigma}}\right)\psi & -\mu\Phi_\kappa\psi & \frac{H'\mu\Phi}{\tilde{\sigma}} \\ \frac{3\tilde{\tau}}{\tilde{\sigma}}\left(\frac{2\Phi}{\tilde{\sigma}} - \mu\Phi_{\tilde{\sigma}}\right)\psi & -\Phi_\kappa\psi^2 & \frac{2H'\Phi\psi}{\tilde{\sigma}} \end{bmatrix} \stackrel{\text{def}}{=} -\mathbf{\Lambda},$$

where

$$\mu\Phi = \frac{\tilde{\sigma} - \sigma_Y - H''\kappa}{H\beta + R(\beta - \tilde{\sigma} + \sigma_Y + H''\kappa)},$$

$$\mu\Phi_{\tilde{\sigma}} = \frac{(R+H)\beta}{[H''\beta + (R+H')(\beta - \tilde{\sigma} + \sigma_Y + H''\kappa)][H\beta + R(\beta - \tilde{\sigma} + \sigma_Y + H''\kappa)]},$$

$$\Phi_\kappa = -H''\Phi_{\tilde{\sigma}}.$$

Let $\mathbf{u} \stackrel{\text{def}}{=} (\tilde{\sigma}, \kappa, \gamma^p)$ and $\mathbf{g}(\tau, \mathbf{u}) \stackrel{\text{def}}{=} (\psi, \theta, \chi)$. If $\mathbf{u} = \mathbf{u}_i$ has been evaluated at $\tau = \tau_i$, and if $\tau_{i+1} = \tau + \Delta\tau$, then the generalized Euler method leads to

$$\mathbf{u}_{i+i} = \mathbf{u}_i + [\mathbf{1} + \alpha\Delta\tau\mathbf{\Lambda}(\tau_i, \mathbf{u}_i)]^{-1}[(1-\alpha)\mathbf{g}(\tau_i, \mathbf{u}_i) + \alpha\mathbf{g}(\tau_{i+1}, \mathbf{u}_i)],$$

where $\mathbf{1}$ is the 3×3 unit matrix.

In the case of purely kinematic hardening ($H' = H$, $H'' = 0$), the problem is simplified because the right-hand sides of eqns (22) are independent of κ and therefore the second equation becomes unnecessary. Computations show that the results are once again virtually independent of α, and no discernible difference is found between results obtained with an increment in τ of 0.16 and one of 0.016. Plots of τ against γ, analogous to those of Fig. 3, are shown in Fig. 4. Note that the curves corresponding to different values of σ, unlike

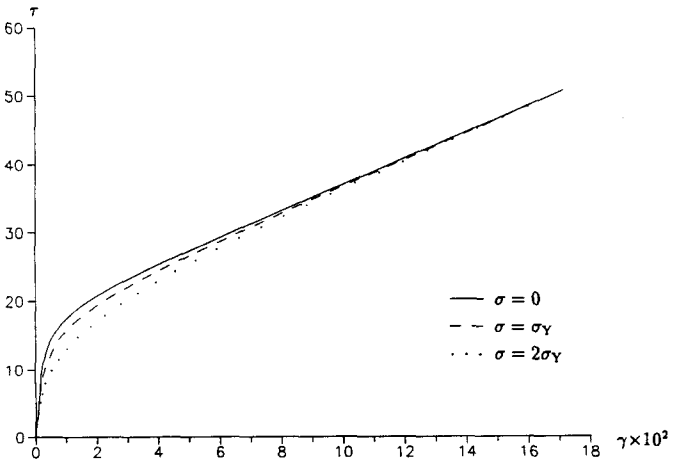

Fig. 4. Torsion of a thin-walled tube under constant axial force, purely kinematic hardening.

those of Fig. 3 for purely isotropic hardening, do not cross; instead, the effect of axial force disappears after a sufficient amount of twist.

3.4. *Combined hardening under strain control*

Since $\boldsymbol{\nu}:\dot{\boldsymbol{\sigma}} = \boldsymbol{\nu}:\dot{\mathbf{s}} = 2G\boldsymbol{\nu}:(\dot{\mathbf{e}}-\dot{\boldsymbol{\varepsilon}}^{\mathrm{p}})$ and, for the von Mises criterion, $\boldsymbol{\nu}:\dot{\boldsymbol{\varepsilon}}^{\mathrm{p}} = \frac{3}{2}\dot{\kappa}$, it follows from eqn (8) that

$$\dot{\kappa} = 2G\phi\langle \boldsymbol{\nu}:\dot{\mathbf{e}} - \tfrac{3}{2}\dot{\kappa}\rangle,$$

so that eqn (8) may be replaced by

$$\dot{\boldsymbol{\varepsilon}}^{\mathrm{p}} = \frac{3}{2}\frac{3G\phi}{(1+3G\phi)\tilde{\sigma}^2}\tilde{\mathbf{s}}\langle\tilde{\mathbf{s}}:\dot{\boldsymbol{\varepsilon}}\rangle, \tag{23}$$

where $\tilde{\mathbf{s}}$ may now be defined as

$$\tilde{\mathbf{s}} = 2(G\mathbf{e} - G'\boldsymbol{\varepsilon}^{\mathrm{p}}),$$

with $G' = G + \frac{1}{3}H'$. Note that

$$\frac{3G\phi}{1+3G\phi} = \frac{3G\langle f\rangle}{(R+H)\beta+(3G-R)f} \overset{\text{def}}{=} \zeta(\tilde{\sigma},\kappa).$$

If $\bar{\varepsilon}$ is defined by

$$\mathrm{d}\bar{\varepsilon} = |\mathrm{d}\boldsymbol{\varepsilon}|$$

and if $\mathrm{d}\boldsymbol{\varepsilon} = \boldsymbol{\eta}\,\mathrm{d}\bar{\varepsilon}$, then, with $\bar{\varepsilon}$ as the independent variable, the differential equations are

$$\begin{aligned}
\frac{\mathrm{d}\tilde{\sigma}}{\mathrm{d}\bar{\varepsilon}} &= \frac{3(G-G'\zeta)}{2\tilde{\sigma}}\langle\tilde{\mathbf{s}}:\boldsymbol{\eta}\rangle,\\
\frac{\mathrm{d}\kappa}{\mathrm{d}\bar{\varepsilon}} &= \frac{\zeta}{\tilde{\sigma}}\langle\tilde{\mathbf{s}}:\boldsymbol{\eta}\rangle,\\
\frac{\mathrm{d}\boldsymbol{\varepsilon}^{\mathrm{p}}}{\mathrm{d}\bar{\varepsilon}} &= \frac{3\zeta}{2\tilde{\sigma}^2}\tilde{\mathbf{s}}\langle\tilde{\mathbf{s}}:\boldsymbol{\eta}\rangle.
\end{aligned} \tag{24}$$

These are not fundamentally different from (19)–(21), and may be attacked by similar methods of solution. As under stress control, in the case of purely kinematic hardening the equation for κ is superfluous. However, purely isotropic hardening under strain control does not entail the same kind of simplification that it does under stress control.

4. APPLICATION OF RETURN-MAP ALGORITHM

4.1. *Derivation of algorithm*

The *return-map algorithm*, initially suggested by Maenchen and Sack (1964) and Wilkins (1964), provides an efficient and robust integration scheme in a finite-element setting for problems in classical plasticity governed by the von Mises criterion and its associated flow rule. It is based on a discrete enforcement of the yield inequality $f \leqslant 0$, and is a two-part algorithm belonging to the elastic-predictor/plastic-corrector family. In the first part, a purely elastic *trial state* is computed; in the second part, if the trial state violates any of the consitutive equations, a correction is computed and applied in such a manner that the final state is consistent with the discrete constitutive model. The algorithm has been widely studied (Nagtegaal, 1982; Simo and Taylor, 1985, 1986; Ortiz and Simo, 1986), as have its accuracy and stability (Ortiz and Popov, 1985; Simo and Govindjee, 1991).

Simo and Hughes (1988) have shown that the algorithm may be extended to other constitutive models, such as viscoplasticity, if the yield inequality is replaced by a *limit inequality*, say $g \leqslant 0$, and that it is equivalent to the closest-point projection of the trial state to the *limit surface* $g = 0$. An extension to generalized plasticity was derived by Auricchio *et al.* (1991, 1992), and will be outlined below.

It follows from eqns (10) that

$$\phi \mathbf{v} : \dot{\boldsymbol{\sigma}} - \dot{\kappa} \leqslant 0. \tag{25}$$

This inequality may be defined as the limit inequality for generalized plasticity. As a result of the developments in Section 2.2, it may be rewritten as

$$\phi(\dot{\tilde{\sigma}} + H'\dot{\kappa}) - \dot{\kappa} \leqslant 0. \tag{26}$$

By combining eqns (8) and (10), we obtain

$$\dot{\boldsymbol{\varepsilon}}^{\mathrm{p}} = \dot{\kappa}\mathbf{v}, \tag{27}$$

so that κ, aside from being the isotropic hardening variable, may also serve as something like the consistency parameter of classical plasticity theory. If eqn (27) is approximately integrated from t_i to t_{i+1} by the backward Euler method, and if for any time-dependent function $\mathbf{a}(t)$ we write, for simplicity, $\mathbf{a}$ for $\mathbf{a}_{i+1}$, then

$$\boldsymbol{\varepsilon}^{\mathrm{p}} = \boldsymbol{\varepsilon}_i^{\mathrm{p}} + \lambda \mathbf{v}, \tag{28}$$

where

$$\lambda = \kappa - \kappa_i = \int_{t_i}^{t_{i+1}} \dot{\kappa}\, \mathrm{d}t$$

is computed by means of the integration algorithm. It follows further that

$$\mathbf{s} = 2G(\mathbf{e} - \boldsymbol{\varepsilon}_i^{\mathrm{p}} - \lambda \mathbf{v}) \tag{29}$$

and

$$\tilde{\mathbf{s}} = 2G(\mathbf{e} - \boldsymbol{\varepsilon}_i^{\mathrm{p}} - \lambda \mathbf{v}) - \tfrac{2}{3}H'(\boldsymbol{\varepsilon}_i^{\mathrm{p}} + \lambda \mathbf{v}). \tag{30}$$

When the limit inequality is also integrated from t_i to t_{i+1} by the backward Euler method, the result is

$$\phi(\tilde{\sigma} - \tilde{\sigma}_i + H'\lambda) - \lambda \leqslant 0. \tag{31}$$

The two steps of the algorithm are as follows:

- *Trial state*: it is assumed that no plastic deformation occurs during the interval $[t_i, t_{i+1}]$, so that $\lambda = 0$. Consequently

$$\boldsymbol{\varepsilon}^{\mathrm{p,tr}} = \boldsymbol{\varepsilon}_i^{\mathrm{p}},$$

$$\mathbf{s}^{\mathrm{tr}} = 2G(\mathbf{e} - \boldsymbol{\varepsilon}_i^{\mathrm{p}})$$

and

$$\tilde{\mathbf{s}}^{\mathrm{tr}} = 2G(\mathbf{e} - \boldsymbol{\varepsilon}_i^{\mathrm{p}}) - \tfrac{2}{3}H'\boldsymbol{\varepsilon}_i^{\mathrm{p}},$$

from which $\tilde{\sigma}^{\mathrm{tr}}$ can be calculated. If the trial state does not violate the integrated limit inequality (31), which reduces to $\tilde{\sigma}^{\mathrm{tr}} \leqslant \tilde{\sigma}_i$, then this state represents the solution at t_{i+1} and the second part of the algorithm can be skipped.

- *Plastic correction*: If $\tilde{\sigma}^{tr} > \tilde{\sigma}_i$, then λ must be computed from eqn (31) as an equality. Equations (29) and (30) can then be rewritten in terms of the trial state and λ:

$$\mathbf{s} = \mathbf{s}^{tr} - 2G\lambda \mathbf{v},$$
$$\tilde{\mathbf{s}} = \tilde{\mathbf{s}}^{tr} - (2G + \tfrac{2}{3}H')\lambda \mathbf{v}.$$

It follows from eqn (9) that $\tilde{\mathbf{s}}^{tr}$ is also parallel to $\mathbf{v}$, so that we have

$$\tilde{\mathbf{s}} = \tfrac{2}{3}\tilde{\sigma}\mathbf{v}, \tag{32}$$

$$\tilde{\mathbf{s}}^{tr} = \tfrac{2}{3}\tilde{\sigma}^{tr}\mathbf{v} \tag{33}$$

and hence

$$\mathbf{v} = \mathbf{v}^{tr}. \tag{34}$$

The following relation between $\tilde{\sigma}$ and $\tilde{\sigma}^{tr}$ can now be obtained:

$$\tilde{\sigma} = \tilde{\sigma}^{tr} - (3G + H')\lambda. \tag{35}$$

Equations (32)–(35) constitute the return-map algorithm.

When the expression (35) for $\tilde{\sigma}$, along with the relation $\kappa = \kappa_i + \lambda$, is used in the expression (7) for f, and that in turn is substituted for f (assumed non-negative) in eqn (6), the following expression is obtained for ϕ:

$$\phi = \frac{A_1 - 3G'\lambda}{(R+H)\beta - RA_1 + 3G'R\lambda},$$

where $H = H' + H''$ and $G' = G + \frac{1}{3}H$ as before, and

$$A_1 = \tilde{\sigma}^{tr} - \sigma_Y - H''\kappa_i.$$

Inserting this expression for ϕ into eqn (31) as an equality results in a quadratic equation for λ,

$$a\lambda^2 + b\lambda + c = 0, \tag{36}$$

where, with the additional definition

$$A_2 = \tilde{\sigma}^{tr} - \tilde{\sigma}_i,$$

the coefficients are

$$a = 3G'(R - 3G),$$
$$b = (R+H)\beta + 3G'A_2 - (R - 3G)A_1,$$
$$c = -A_1 A_2.$$

The physically correct solution corresponds to the smallest positive root of (36).

4.2. *Numerical examples*

The method based on the return-map algorithm was subjected to numerical tests in the finite-element context using a three-dimensional isoparametric element, based on a mixed approach (Simo *et al.*, 1985) and incorporated in the Finite Element Analysis Program [FEAP, Zienkiewicz and Taylor (1989, 1991)]. A consistent linearization of the

return map algorithm as described in Auricchio *et al.* (1991, 1992) is used to construct the tangent matrix. The following examples were considered:

- Uniaxial stress.
- Thin-walled tube under tension and torsion.
- Thick-walled tube under internal pressure.

Uniaxial stress was modeled by a cubic specimen, forming a single element, with boundary conditions and loading set so as to produce a state of uniaxial stress. Both a simple loading–unloading history and a cyclic loading history were run. The results are undistinguishable from those obtained by direct integration of the uniaxial rate equations.

The thin-walled tube under combined tension and torsion was studied under both stress and displacement control. The tests under stress control are equivalent to those considered in Section 3, and the results are again undistinguishable from those shown in Figs 3 and 4. In the displacement–control problem, the tube is initially (from $t = 0$ to $t = 10$) extended axially past the yield limit, and then twisted with the axial displacement maintained constant. With material properties given by

$$E = 300, \quad \nu = 0.3, \quad \sigma_Y = 10,$$
$$R = 30, \quad \beta = 5, \quad H = 0,$$

the axial stress and shear stresses are plotted against time in Figs 5 and 6. For comparison,

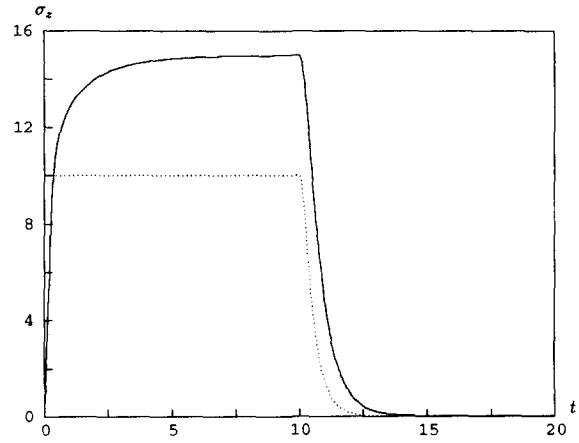

Fig. 5. Thin-walled tube under tension and torsion (displacement control): axial stress history (dotted curve: classical plasticity result, analytical and numerical).

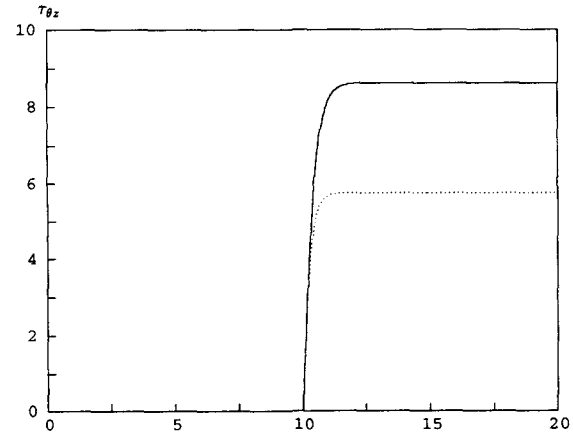

Fig. 6. Thin-walled tube under tension and torsion (displacement control): tangential shear-stress history (dotted curve: classical plasticity result, analytical and numerical).

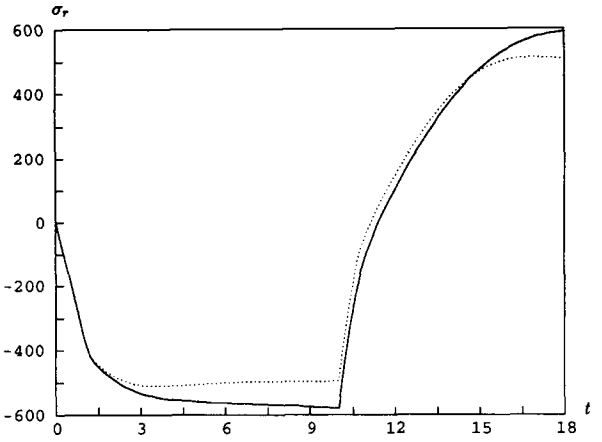

Fig. 7. Thick-walled tube under internal pressure (displacement control): pressure history (dotted curve: result for $\beta = 0$, i.e. classical plasticity).

computations for $\beta = 0$, corresponding to classical plasticity (and in which case the results are independent of R), are also shown; these results are undistinguishable from those derived analytically [see, e.g., Lubliner (1990)].

As the final example, we consider a long thick-walled cylinder subjected to an internal pressure loading. The inner and the outer radii of the cylinder are 2 and 10, respectively. The material properties are

$$E = 10^6, \quad \nu = 0.3, \quad \sigma_Y = 10^3,$$
$$R = 10^3, \quad \beta = 500, \quad H = 0.$$

The internal pressure effects are simulated by controlling the displacement of the inner surface and, as a result, the loading history is expressed in terms of this quantity. The displacement is increased linearly in time from 0 at $t = 0$ to 20 at $t = 10$, and then linearly decreased back to zero at $t = 20$. The radial stress on the inner surface is plotted against time in Fig. 7. The solution for classical plasticity ($\beta = 0$) is also shown for comparison.

REFERENCES

Auricchio, F., Taylor, R. L. and Lubliner, J. (1991). Application of a return map algorithm to plasticity and visco-plasticity models. Report No. UCB/SEMM 91/08, Department of Civil Engineering, University of California, Berkeley, CA.

Auricchio, F., Taylor, R. L. and Lubliner, J. (1992). Application of a return map algorithm to plasticity models. In *Computational Plasticity: Fundamentals and Applications* (Edited by D. R. J. Owen, E. Oñate and E. Hinton), pp. 2229–2248. Pineridge Press, Swansea, NJ..

Dahlquist, G. and Björck, Å. (1974). *Numerical Methods* (tr. N. Anderson). Prentice-Hall, Englewood Cliffs, NJ.

Lubliner, J. (1974). A simple theory of plasticity. *Int. J. Solids Structures* **10,** 313–319.

Lubliner, J. (1975). On loading, yield and quasi-yield hypersurfaces in plasticity theory. *Int. J. Solids Structures* **11,** 1011–1016.

Lubliner, J. (1980). An axiomatic model of rate-independent plasticity. *Int. J. Solids Structures* **16,** 709–713.

Lubliner, J. (1981). Plasticity and ultimate strength of concrete. In *Physical Non-Linearities in Structural Analysis* (Edited by J. Hult and J. Lemaitre), pp. 160–164. Springer, Berlin.

Lubliner, J. (1984). A maximum-dissipation principle in generalized plasticity. *Acta Mech.* **52,** 225–237.

Lubliner, J. (1989). Some simple models of generalized plasticity. In *Advances in Plasticity 1989* (Edited by A. S. Khan and M. Tokuda), pp. 637–641. Pergamon Press, Oxford.

Lubliner, J. (1990). *Plasticity Theory*. Macmillan, New York.

Lubliner, J. (1991). A simple model of generalized plasticity. *Int. J. Solids Structures* **28,** 769–778.

Maenchen, G. and Sack, S. (1964). The tensor code. In *Methods in Computational Physics* (Edited by B. Alder), Vol. 3, pp. 181–210. Academic Press, New York.

Nagtegaal, J. C. (1982). On the implementation of inelastic constitutive equations with special attention to large-deformation problems. *Comput. Meth. Appl. Mech. Engng* **33,** 469–484.

Ortiz, M. and Popov, E. P. (1985). Accuracy and stability of integration algorithms for elastoplastic constitutive relations. *Int. J. Numer. Meth. Engng* **21,** 1561–1576.

Ortiz, M. and Simo, J. C. (1986). An analysis of a new class of integration algorithms for elastoplastic constitutive relations. *Int. J. Numer. Meth. Engng* **23,** 353–366.

Simo, J. C. and Govindjee, S. (1991). Non linear B stability and symmetry preserving return mapping algorithms for elastoplastic constitutive relations. *Int. J. Numer. Meth. Engng* **31,** 151–176.

Simo, J. C. and Hughes, T. J. R. (1988). Elasticity and viscoplasticity: Computational aspects. Department of Applied Mechanics, Stanford University.

Simo, J. C. and Taylor, R. L. (1985). Consistent tangent operators for rate-independent elastoplasticity. *Comput. Meth. Appl. Mech. Engng* **48,** 101–118.

Simo, J. C. and Taylor, R. L. (1986). A return mapping algorithm for plane stress elastoplasticity. *Int. J. Numer. Meth. Engng* **22,** 649–670.

Simo, J. C., Taylor, R. L. and Pister, K. S. (1985). Variational and projection methods for the volume constraint in finite deformation elastoplasticity. *Comput. Meth. Appl. Mech. Engng* **51,** 177–208.

Wilkins, M. L. (1964). Calculation of elastic–plastic flow. In *Methods in Computational Physics* (Edited by B. Alder), Vol. 3, pp. 211–263. Academic Press, New York.

Zienkiewicz, O. C. and Taylor, R. L. (1989). *The Finite Element Method* (4th Edn), Vol. I. McGraw-Hill, London.

Zienkiewicz, O. C. and Taylor, R. L. (1991). *The Finite Element Method* (4th Edn), Vol. II. McGraw-Hill, London.